

Calorimetric and x-ray diffraction studies of α -to- β structural phase transitions in HfW_2O_8 and ZrW_2O_8

Y. Yamamura, N. Nakajima, and T. Tsuji*

Center for New Materials, Japan Advanced Institute of Science and Technology, 1-1 Asahidai, Tatsunokuchi, Ishikawa 923-1292, Japan

(Received 6 September 2000; published 19 October 2001)

A powder x-ray diffraction experiment was performed on cubic HfW_2O_8 and ZrW_2O_8 from 90 to 560 K. The lattice parameter and absolute negative thermal expansion coefficient of HfW_2O_8 are smaller than those of ZrW_2O_8 . The heat capacity of HfW_2O_8 was measured from 340 to 520 K using an adiabatic scanning calorimeter. An anomaly in heat capacity of HfW_2O_8 corresponding to the α -to- β structural phase transition was clearly detected around 463 K. The phase transition temperature of HfW_2O_8 by the calorimeter is 26 K higher than that of ZrW_2O_8 . The entropy of transition of HfW_2O_8 is the same magnitude as that of ZrW_2O_8 , indicating that the mechanism of the phase transition of HfW_2O_8 and ZrW_2O_8 is the same.

DOI: 10.1103/PhysRevB.64.184109

PACS number(s): 64.60.-i, 65.40.-b, 65.40.De

I. INTRODUCTION

A lot of studies on zirconium tungsten oxide, ZrW_2O_8 , have been carried out in the past several years. ZrW_2O_8 is an isotropic compound with a negative thermal expansion over a wide temperature range from 4 to 1050 K.¹⁻³ This interesting feature of ZrW_2O_8 is closely related to its rare crystal structure. ZrW_2O_8 belongs to the cubic system with a cell parameter $a = 0.91568$ nm at room temperature² and the unit cell contains four chemical formula units. The crystal has a framework structure that is characterized by linkages of the corner shared WO_4 tetrahedra and ZrO_6 octahedra. The linkage is such that the ZrO_6 octahedral units share all corners with six WO_4 tetrahedral units. On the other hand, each WO_4 unit shares only three of its four oxygens with the adjacent ZrO_6 units. The other oxygen of each WO_4 unit is, therefore, bound to only one W atom and is an unshared vortex of the WO_4 tetrahedron. The framework structure and the liberation of the WO_4 unit with the unshared vortex result in the nature of negative thermal expansion.^{4,5}

ZrW_2O_8 undergoes a structural phase transition at about 430 K from an acentric to a centric structure with increasing temperature.^{1,2} The structural phase transition is related to the orientation of the unshared vortex of WO_4 unit. In the low temperature phase (α -phase, $P2_13$), the two WO_4 tetrahedra point their unshared vertexes to the $[111]$ direction, whereas randomly to $[111]$ or $-[111]$ directions with the ratio 1:1 in the high temperature phase (β -phase, $Pa\bar{3}$).^{1,2} The structural phase transition of ZrW_2O_8 is therefore of order-disorder type. In this order-disorder phase transition, it was suggested from structural and thermodynamic considerations that these two WO_4 tetrahedra on the $[111]$ body diagonal change their orientation concertedly.^{1,2,6} Two possible disordering processes have been proposed so far. One is an inverting process accompanied with the migration of the oxygen ion that is the terminal oxygen of WO_4 tetrahedron.^{1,2} The other is a process without breaking the bond between the terminal oxygen and tungsten atom in WO_4 tetrahedron.⁷ The former process is, however, supported by the movement of oxygen ions at α -to- β phase

transition⁸ and also the temperature and frequency dependence of ion conductivity.²

Hafnium tungsten, HfW_2O_8 , is isostructural to ZrW_2O_8 and shows the thermal contraction similar to ZrW_2O_8 .^{1,2,9} It is well known that zirconium and hafnium elements resemble each other in chemical properties, in spite of a large difference in the atomic number of 32. Further, the two elements have nearly the same ionic radius because of lanthanide contraction for hafnium:¹⁰ An ionic radius of Zr^{4+} with six coordination is 86 pm and that of Hf^{4+} is 85 pm.¹¹ In spite of this, ZrO_2 , which is a famous oxide including zirconium, shows larger lattice constants¹² and lower phase transition temperature from monoclinic to tetragonal phase having higher symmetry than that of HfO_2 .¹³ This fact suggests that a small difference in properties between Zr and Hf atoms leads to different physical properties of their oxides. Sleight and co-workers^{1,2} stated in their several papers that physical properties of HfW_2O_8 were nearly the same as those of ZrW_2O_8 concerning a negative thermal expansion and phase transition. Only negative thermal expansion datum by thermomechanical analysis (TMA) was, however, reported for HfW_2O_8 in detail.⁹

In this paper, we report structural properties on HfW_2O_8 and ZrW_2O_8 by using powder x-ray diffractometry. Calorimetric study on HfW_2O_8 was also carried out, and thermodynamic data obtained are compared with those of ZrW_2O_8 .

II. EXPERIMENT

HfW_2O_8 was prepared by a conventional solid-state reaction.⁶ A stoichiometric amount of hafnium oxide (purity 99.95%, Rare Metallic Co., Ltd.) and tungsten trioxide (purity 99.99%, Kojundo Chemical Laboratory Co., Ltd.) was mixed in an agate mortar and made into pellets. The pellets were calcined at 1473 K for 12 h in air and then rapidly cooled down to room temperature. The calcined pellets were ground well and pressed into pellets again. The pellets were sintered at 1473 K for 12 h in air and then quenched in liquid nitrogen.

The samples of HfW_2O_8 and ZrW_2O_8 were characterized by x-ray powder diffractometer using $\text{Cu } K\alpha$ radiation with

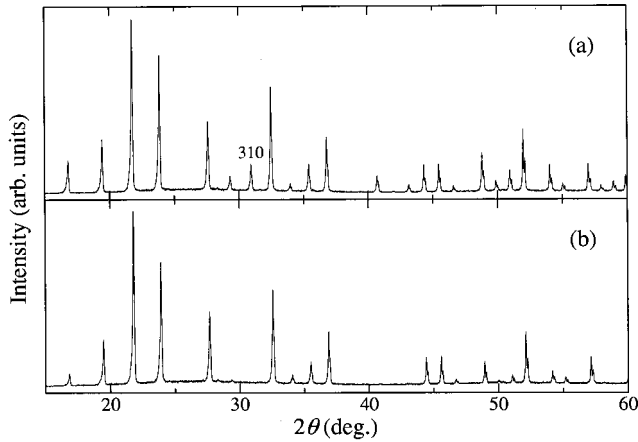


FIG. 1. X-ray diffraction patterns of HfW_2O_8 at room temperature (a) and 558 K (b).

40 kV–200 mA (RINT 2500V, Rigaku), having low and high temperature attachments capable of controlling temperature within ± 1 K. The XRD data were collected by a step-scanning method in the 2θ range from 10 to 100° with a step width of 0.01° and a scan time of 0.7 s. The powder patterns ($2\theta = 10\text{--}100$) were obtained at about 35 temperatures from 90 to 560 K in a vacuum environment. Temperature was kept at constant for about 20 min before x-ray diffraction measurement at each temperature.

The heat capacity of HfW_2O_8 was measured using an adiabatic scanning calorimeter (ASC) from 340 to 520 K. Details of the apparatus and the operation of the ASC have been described elsewhere.¹⁴ The crushed sample of HfW_2O_8 was loaded into a quartz ampul as a calorimeter vessel and sealed with a small amount of helium gas (20 kPa at room temperature) to assist thermal equilibration within the ampul. The amount of the sample used for the measurement was about 16 g. Before heat capacity measurement, the ampul with the sample was annealed at about 800 K for one hour, in order to remove the quenching effects in the sample preparation. The heating rate (scanning rate) chosen in this study was about 1.8 K min^{-1} . A preliminary heat capacity measurement of sapphire using the ASC showed that a precision and an accuracy of the calorimeter were within $\pm 2\%$ and $\pm 2\%$, respectively, in comparison with the reliable data of sapphire.¹⁵

III. RESULTS AND DISCUSSION

The sample of HfW_2O_8 was characterized to be of single phase by a powder x-ray diffraction method. The powder pattern of HfW_2O_8 at room temperature shown in Fig. 1(a) is the same as the previous reports^{9,16} and very similar to that of ZrW_2O_8 .^{2,9} The diffraction peaks in the powder pattern were assigned by referring to the previous work for ZrW_2O_8 by Sleight's group.² A lattice parameter of HfW_2O_8 was determined using about 40 diffractions between 40 and 100° by a least-square calculation after correcting of 2θ with Nelson-Riley's method.¹⁷ The lattice parameter of HfW_2O_8 at room temperature is $0.9131(1) \text{ nm}$, which is comparable to the

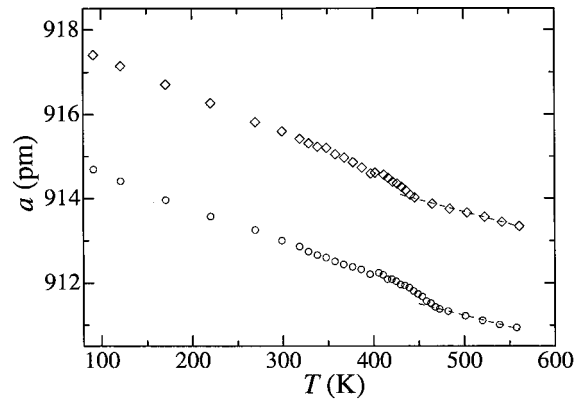


FIG. 2. Lattice parameters of HfW_2O_8 (\circ) and ZrW_2O_8 (\diamond) as a function of temperature. The broken lines at higher temperatures are calculated by a least-square method.

previous report (0.913 nm).¹⁶ On the other hand, the lattice parameter [$0.9157(1) \text{ nm}$] of ZrW_2O_8 is 0.0026 nm larger than that of HfW_2O_8 . This distinction is attributed to a difference in ionic radius between Zr^{4+} (86 pm) and Hf^{4+} (85 pm) ions.

Figure 1(b) shows the powder x-ray pattern of HfW_2O_8 at 558 K. A few diffraction peaks in Fig. 1(b), for example (310) peak, are absent in comparison with the powder pattern at room temperature shown in Fig. 1(a). The indices of the disappearing peaks in HfW_2O_8 are identical to those in ZrW_2O_8 on the α -to- β phase transition. This disappearance, therefore, suggests that HfW_2O_8 also undergoes the α -to- β phase transition above room temperature. To compare lattice parameters of HfW_2O_8 with those of ZrW_2O_8 , powder x-ray diffraction experiments on HfW_2O_8 and ZrW_2O_8 were carried out at about 35 temperatures from 90 to 560 K. At all the temperatures, the lattice parameters of both HfW_2O_8 and ZrW_2O_8 were determined by the same manner as described at room temperature above. Figure 2 shows the lattice parameters of HfW_2O_8 and ZrW_2O_8 as a function of temperature. Our results on ZrW_2O_8 agree quite well with the reported values by Sleight's group.^{1–3} The lattice parameters of HfW_2O_8 are smaller than those of ZrW_2O_8 over the whole temperature range covered in this study, reflecting a difference in ionic radius between Zr^{4+} and Hf^{4+} ions. Figure 2 shows that the temperature dependence of the lattice parameter of HfW_2O_8 is very similar to that of ZrW_2O_8 . There are anomalies in the lattice parameters of both ZrW_2O_8 and HfW_2O_8 . These anomalies are due to the α -to- β phase transition as discussed above. The temperature dependence of lattice parameters in both materials is continuous around the phase transition temperature. These curves are, however, unusual in comparison with a general continuous phase transition, where the curve of lattice parameter bents at the phase transition temperature. The phase transition temperatures were determined from both the temperature of disappearance of (310) diffraction peak and the temperature where the lattice parameter curve of α -phase reached the extrapolated line of the lattice parameters in β -phase (see broken lines in Fig. 2). The phase transition temperature of HfW_2O_8 is $468 \pm 2 \text{ K}$, while that of ZrW_2O_8 is $444 \pm 2 \text{ K}$ which is in good

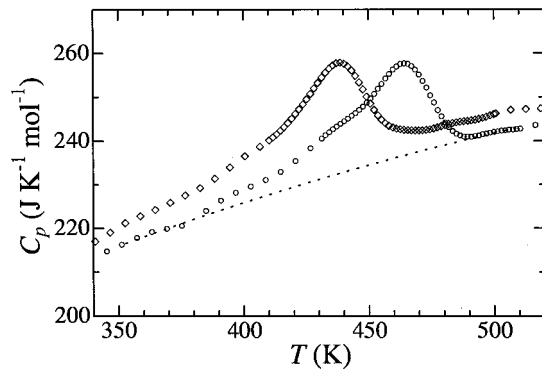


FIG. 3. Heat capacities of HfW_2O_8 (\circ) and ZrW_2O_8 (\diamond) as a function of temperature. The broken line is a baseline used to estimate the excess heat capacity for HfW_2O_8 .

agreement with the previous datum (448 K).³ It means that the phase transition temperature is 24 K higher in HfW_2O_8 than ZrW_2O_8 .

The thermal expansion coefficients of HfW_2O_8 were determined from Fig. 2 as about $-8.8 \times 10^{-6} \text{ K}^{-1}$ (90–300 K) and about $-5.5 \times 10^{-6} \text{ K}^{-1}$ (500–560 K) for the low and the high temperature phases, respectively. On the other hand, those of ZrW_2O_8 were about $-9.6 \times 10^{-6} \text{ K}^{-1}$ (90–300 K) in α -phase and about $-6.2 \times 10^{-6} \text{ K}^{-1}$ (500–560 K) in β -phase. HfW_2O_8 shows slightly smaller absolute thermal expansion coefficients than ZrW_2O_8 in both α and β phases.

In Fig. 2, a small irregularity can be seen in the experimental curves of both ZrW_2O_8 and HfW_2O_8 at about 410 K. There is, however, no change in their diffraction patterns around that temperature. The small irregularity is probably due to the annealing effect stated in Ref. 3, where if the temperature was kept at 386 K for 4 h, an increase in lattice parameter was observed in ZrW_2O_8 . In this XRD study, since the temperature was kept at a constant for more than 2 h on every measurement, the annealing effect may cause this small irregularity in lattice parameter as a function of temperature.

In order to get further information concerning thermodynamic properties on HfW_2O_8 , a calorimetric experiment was performed from 340 to 520 K by an adiabatic scanning calorimeter (ASC). Figure 3 shows heat capacity, C_p , of HfW_2O_8 as a function of temperature, together with the previous heat capacity data of ZrW_2O_8 by the present authors.⁶ Curiously, the magnitude of heat capacity before and after peak of HfW_2O_8 is smaller than that of ZrW_2O_8 ,⁶ in spite of the larger mass of Hf than Zr. This inversion in the heat capacity value between HfW_2O_8 and ZrW_2O_8 has been definitely confirmed in adiabatic calorimetric measurements at Osaka University,¹⁸ where heat capacity data are reliable within 1 percent in absolute magnitude. The inversion of the heat capacity may result from a difference in frequency of high-energy optical phonon modes between Zr-O and Hf-O. The lattice parameters and the ionic radii suggest that the Hf-O bond is shorter and stronger than Zr-O one, leading to the higher energy of the stretching vibrational modes of Hf-O than those of Zr-O. In this case, it is possible that the

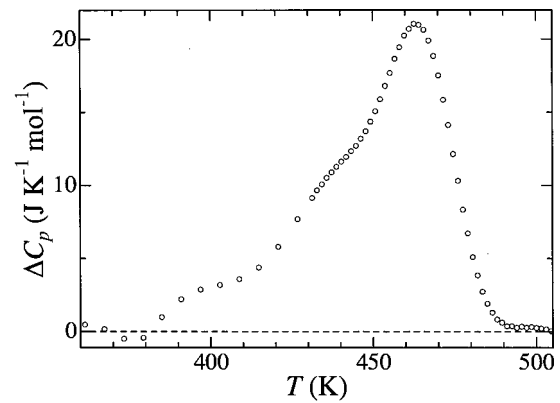


FIG. 4. Excess heat capacity due to α -to- β order-disorder phase transition in HfW_2O_8 as a function of temperature.

vibrational modes of Hf-O have smaller contributions to the heat capacity than those of Zr-O at the same temperature. A more detailed discussion will appear elsewhere.¹⁸ Those facts demonstrate the inadequacy of the statement that physical properties of two compounds are almost identical, as pointed out by Sleight's group.^{1,2} The difference in heat capacities of both compounds is even more our "classical understandings" on them.

There is an anomalous peak of heat capacity of HfW_2O_8 at about 460 K in Fig. 3. The temperature range of the anomaly in heat capacity seems to correspond to that of the anomaly in the results from x-ray experiments. The anomaly is, therefore, attributed to the α -to- β structural phase transition. The shape of the anomaly of HfW_2O_8 is very similar to that of ZrW_2O_8 ,⁶ but the anomalous peak of heat capacity for HfW_2O_8 is 26 K higher than that of ZrW_2O_8 . In addition, it is very interesting to note that, if the entire heat capacity of ZrW_2O_8 shifts to higher temperature by 26 K, the heat capacity curve of ZrW_2O_8 (Ref. 6) matches with that of HfW_2O_8 . For more detailed discussion on the thermodynamic properties of the phase transition, it is necessary to separate the excess heat capacity due to the phase transition from the total heat capacity by determining a baseline. In general, the baseline may be determined by interpolating heat capacities in both higher- and lower-temperature ranges excluding the phase transition region. For the base line of ZrW_2O_8 in the previous work,⁶ the heat capacities in the temperature regions above 480 K and below 330 K have been adopted. The base line in higher temperature region for HfW_2O_8 can be obtained from the heat capacity data above about 505 K. On the other hand, the base line in lower temperature region seems to be the heat capacity below about 370 K. A smooth interpolating curve, as shown by the broken line in Fig. 3, was thus estimated in consistency with the result on ZrW_2O_8 . The excess heat capacities are obtained by subtracting the baseline shown in Fig. 3 from the total heat capacity and plotted in Fig. 4. The shape of the excess heat capacity is remarkably similar to that of ZrW_2O_8 (Ref. 6) and is regarded as λ -type, which is a general shape of the second-order phase transition. Accordingly, the phase transition of HfW_2O_8 is of second (or higher) order as in the case of

TABLE I. Thermodynamic data of ZrW_2O_8 and HfW_2O_8 .

	$T_{\text{trs}}/\text{K}(\text{XRD})$	$T_{\text{trs}}/\text{K}(\text{ASC})$	$\Delta_{\text{trs}}H/\text{J mol}^{-1}$	$\Delta_{\text{trs}}S/\text{J K}^{-1} \text{mol}^{-1}$
ZrW_2O_8	444 ± 2	437 ± 1	907 ± 10	2.1 ± 0.2
HfW_2O_8	468 ± 2	463 ± 1	934 ± 10	2.1 ± 0.2

ZrW_2O_8 . This is also supported by the x-ray experiment, which shows the continuous temperature dependence on the lattice parameter around the phase transition temperature as described above.

Numerical integration of the excess heat capacities was carried out between 370 and 505 K. The excess enthalpy ($\Delta_{\text{trs}}H$) and entropy ($\Delta_{\text{trs}}S$) attributable to the phase transition are determined as $934 \pm 10 \text{ J mol}^{-1}$ and $2.1 \pm 0.2 \text{ J K}^{-1} \text{ mol}^{-1}$, respectively. Of course, the magnitudes of $\Delta_{\text{trs}}H$ and $\Delta_{\text{trs}}S$ depend on the choice of baseline, which is not included in the error assessment. The present $\Delta_{\text{trs}}H$ and $\Delta_{\text{trs}}S$ should be regarded as the minimum value of the enthalpy and entropy of transition, respectively. It is possible that a depression of the baseline, which extends the temperature range for the integration of the excess heat capacities, leads to larger magnitudes of $\Delta_{\text{trs}}H$ and $\Delta_{\text{trs}}S$. The estimation of true baseline is, however, very hard only in this study, because of a narrow temperature range of the heat capacity data obtained from ASC measurement. T_{trs} (XRD and ASC), $\Delta_{\text{trs}}H$ and $\Delta_{\text{trs}}S$ of HfW_2O_8 are summarized in Table I, together with those of ZrW_2O_8 reevaluated the previous thermodynamic data of ZrW_2O_8 (Ref. 6) by the present authors. The obtained $\Delta_{\text{trs}}S$ ($2.1 \text{ J K}^{-1} \text{ mol}^{-1}$) of HfW_2O_8 coincides with that ($2.1 \text{ J K}^{-1} \text{ mol}^{-1}$) of ZrW_2O_8 within the possible estimated errors. Although the coincidence may be effected from the choice of baseline, this difference of absolute $\Delta_{\text{trs}}S$ values between HfW_2O_8 and ZrW_2O_8 seems to be small because the baselines of both HfW_2O_8 and ZrW_2O_8 are estimated in the same way. This coincidence of the excess entropy suggests that both HfW_2O_8 and ZrW_2O_8 undergo the phase transition with the same order-disorder mechanism, where two WO_4 tetrahedra on [111] diagonal in the unit cell have only two conformations in a concerted manner. This suggestion is not contradictory to the previous reports^{1,2} as well as the x-ray diffraction results described above. The phase transition temperature of HfW_2O_8 corresponding to a maximum of the excess heat capacity was determined to be $463 \pm 1 \text{ K}$ after correction for the scanning effect of ASC measurement. This transition temperature of HfW_2O_8 is 5 K lower than the transition temperature (468 K) obtained by the XRD experiment as described above, in spite of a second (or higher) order phase transition. A similar difference in phase transition temperature is also seen in the case of ZrW_2O_8 (see Table I). In general, a measurement with scanning method, such as ASC, often shows that an apparent temperature of phase transition moves to higher temperature with increasing heating rate. A measurement with high scanning rate by ASC, in fact, showed an increase in the phase transition temperature. The scanning effect is caused by the fact that the sample and the sample holder during the measurement need a finite time to reach thermal equilibrium. From this scan-

ning effect, the phase transition temperature by ASC should be higher than the result by XRD experiment keeping temperature at constant. However, our experimental results for ZrW_2O_8 and HfW_2O_8 are contrary to this scanning effect. Of course, we confirmed that the temperature difference is not caused by the unsatisfactory temperature calibration of the x-ray diffractometry apparatus and the ASC. One probability of the temperature difference is attributed to gas environments around the samples in ASC and XRD equipments. In ASC the sample in the calorimeter vessel is in some He gas to assist quick thermal equilibration. On the other hand, the XRD measurement is carried out under a vacuum environment, where the sample shows poorer thermal conductivity due to larger gas thermal resistance among particles. This different thermal conductivity of the sample between XRD and ASC may lead to the difference in the phase transition temperature. The difference of phase transition temperature between ZrW_2O_8 and HfW_2O_8 is, however, about 25 K in both ASC and XRD. It is noticed that the enthalpy of transition (934 J mol^{-1}) for HfW_2O_8 is larger than that (907 J mol^{-1}) for ZrW_2O_8 , reflecting higher transition temperature of the former than the latter.

Now it is clear that both ZrW_2O_8 and HfW_2O_8 show the same phase transition mechanism, but the different phase transition temperatures. That is, the phase transition temperature of HfW_2O_8 is about 25 K higher than that of ZrW_2O_8 . As mentioned earlier, the different physical quantities between ZrW_2O_8 and HfW_2O_8 are mainly the atomic mass of the constituent atoms and the lattice parameter including the contribution from ionic radius. It is now interesting to note the presence of the previous report on the relation among the composition, the lattice parameter and the phase transition temperature in $\text{ZrW}_{2-x}\text{Mo}_x\text{O}_8$.¹⁹ In this $\text{ZrW}_{2-x}\text{Mo}_x\text{O}_8$ system, the more Mo contents having small atomic mass, the less lattice parameter and the lower temperature of phase transition. When Mo content is over $x=0.7$, the solid solutions take the high-temperature phase (β -phase) even at room temperature. If this relation between the lattice parameter and the phase transition temperature for the $\text{ZrW}_{2-x}\text{Mo}_x\text{O}_8$ solid solution is applied to that for ZrW_2O_8 and HfW_2O_8 , the trend is opposite. On the other hand, if the relation between the formula mass and the phase transition temperature for the $\text{ZrW}_{2-x}\text{Mo}_x\text{O}_8$ solid solution holds, the trend agrees with that for ZrW_2O_8 and HfW_2O_8 . This agreement is very interesting. There is, however, no cogent reason for understanding the agreement. Moreover, it is necessary to consider the difference in the substituted cation sites between $\text{ZrW}_{2-x}\text{Mo}_x\text{O}_8$ and ZrW_2O_8 - HfW_2O_8 systems. In spite of those, to verify the relation among the lattice parameter, the atomic mass and the cation site may lead to understanding

the mechanism of the α -to- β phase transition in AB_2O_8 system.

IV. CONCLUSIONS

The lattice parameters on cubic ZrW_2O_8 and HfW_2O_8 were measured as a function of temperature by powder x-ray diffractometry. The lattice parameter and absolute negative thermal expansion coefficient of HfW_2O_8 are smaller than those of ZrW_2O_8 . Thermodynamic properties on HfW_2O_8 were obtained by calorimetric experiment. Anomalous

changes due to α -to- β structural phase transition of HfW_2O_8 , similar to ZrW_2O_8 , were clearly detected by x-ray diffraction and calorimetric experiments. Since HfW_2O_8 has the same entropy of transition as ZrW_2O_8 , the phase transition of HfW_2O_8 is of order-disorder type, where two WO_4 tetrahedra on [111] diagonal in the unit cell have only two conformations in a concerted manner. Both x-ray and calorimetric experiments show that the phase transition temperature of HfW_2O_8 is about 25 K higher than that of ZrW_2O_8 , probably reflecting stronger chemical bond of Hf-O than Zr-O.

*Author to whom correspondence should be addressed. FAX: +81-761-51-1455. Electronic address: tsuji@jaist.ac.jp

¹T. A. Mary, J. S. O. Evans, T. Vogt, and A. W. Sleight, *Science* **272**, 90 (1996).

²J. S. O. Evans, T. A. Mary, T. Vogt, M. A. Subramanian, and A. W. Sleight, *Chem. Mater.* **8**, 2809 (1996).

³J. S. O. Evans, W. I. F. David, and A. W. Sleight, *Acta Crystallogr., Sect. B: Struct. Sci.* **55**, 333 (1999).

⁴A. P. Ramirez and G. R. Kowach, *Phys. Rev. Lett.* **80**, 4903 (1998).

⁵G. Ernst, C. Broholm, G. R. Kowach, and A. P. Ramirez, *Nature (London)* **396**, 147 (1998).

⁶Y. Yamamura, N. Nakajima, and T. Tsuji, *Solid State Commun.* **114**, 453 (2000).

⁷A. K. A. Pryde, K. D. Hammonds, M. T. Dove, V. Heine, J. D. Gale, and M. C. Warren, *J. Phys.: Condens. Matter* **8**, 10973 (1996); *Phase Transitions* **61**, 141 (1997).

⁸J. S. O. Evans, Z. Hu, J. D. Jorgensen, D. N. Argyriou, S. Short, and A. W. Sleight, *Science* **275**, 61 (1997).

⁹A. W. Slight, T. A. Mary, and J. S. O. Evans, U.S. Patent No. 5514360, 1995.

¹⁰R. B. Heslop and K. Jones, *Inorganic Chemistry* (Elsevier, Amsterdam, 1976).

¹¹R. D. Shannon, *Acta Crystallogr., Sect. A: Cryst. Phys., Diffr., Theor. Gen. Crystallogr.* **A32**, 751 (1976).

¹²R. W. G. Wyckoff, *Crystal Structures*, 2nd ed. (Wiley & Sons, New York, 1965), Vol. 1, p. 244.

¹³T. B. Massalski, J. L. Murray, L. H. Bennett, and H. Baker, *Binary Alloy Phase Diagrams* (American Society for Metals, Metals Park, OH, 1986).

¹⁴K. Naito, N. Kamegashira, N. Yamamda, and J. Kitagawa, *J. Phys. E* **6**, 836 (1973); K. Naito, H. Inaba, M. Ishida, Y. Saito, and H. Arima, *ibid.* **7**, 464 (1974).

¹⁵D. G. Archer, *J. Phys. Chem. Ref. Data* **22**, 1441 (1993).

¹⁶V. K. Trunov and L. M. Kovba, *Russ. J. Inorg. Chem.* **12**, 1703 (1967).

¹⁷J. B. Nelson and D. P. Riley, *Proc. Phys. Soc. London* **57**, 160 (1945).

¹⁸Y. Yamamura, N. Nakajima, T. Tsuji, K. Saito, and M. Sorai (unpublished).

¹⁹C. Closmann, A. W. Sleight, and J. C. Haygarth, *J. Solid State Chem.* **139**, 424 (1998).